Micro-integrated high-power narrow-linewidth external-cavity tapered diode laser at 808 nm

Chi, Mingjun; Müller, André; Hansen, Anders Kragh; Jensen, Ole Bjarlin; Petersen, Paul Michael; Sumpf, Bernd

Published in:
Applied Optics

Link to article, DOI:
10.1364/AO.381439

Publication date:
2020

Document Version
Peer reviewed version

Micro-integrated high-power narrow-linewidth external-cavity tapered diode laser at 808 nm

MINGJUN CHI,[1,*] ANDRÉ. MÜLLER,[2] ANDERS K. HANSEN,[1] OLE B. JENSEN,[1] PAUL M. PETERSEN,[1] AND BERND SUMPF[2]

[1]DTU Fotonik, Department of Photonics Engineering, Technical University of Denmark, Frederiksborgvej 399, P.O. Box 49, DK-4000 Roskilde, Denmark

[2]Ferdinand-Braun-Institut, Leibniz-Institut für Höchstfrequenztechnik, Gustav Kirchhoff-Str.4, 12489 Berlin, Germany

*Corresponding author: mchi@fotonik.dtu.dk

Received XX Month XXXX; revised XX Month, XXXX; accepted XX Month XXXX; posted XX Month XXXX (Doc. ID XXXXX); published XX Month XXXX

A novel compact micro-integrated high-power narrow-linewidth external-cavity diode laser around 808 nm is demonstrated. The laser system contains a tapered amplifier consisting of a ridge-waveguide section and a tapered section with separated electrical contacts. Thus, the injection currents to both sections can be controlled independently. An external volume Bragg grating is utilized for spectral narrowing and stabilization. The diode laser system is integrated on a 5 mm x 13 mm aluminum nitride micro-optical bench on a conduction cooled package mount with a footprint of 25 mm x 25 mm. The diode laser system is characterized by measuring the output power and spectrum with the injection currents to the ridge-waveguide section (I_{RW}) and tapered amplifier section (I_{TA}) changed in steps of 25 and 50 mA, respectively. At I_{RW} = 200 mA and I_{TA} = 6.0 A, 3.5 watts of output power is obtained with an emission spectral linewidth with an upper bound of 6 pm, and a beam propagation factor in the slow axis, M^2, of 2.6 (1/e^2). The characterization of the temperature stabilization of the laser system shows an increase of the wavelength at a rate of 6.5 pm/K, typical for the applied volume Bragg grating.

OCIS codes: (140.5960) Semiconductor lasers; (140.2020) Diode lasers; (090.7330) Volume gratings;

http://dx.doi.org/10.1364/AO.99.099999

1. INTRODUCTION

Narrow-linewidth, high-power and diffraction limited diode lasers in the near infrared spectral range are attractive for many applications such as nonlinear frequency conversion to visible and UV light, solid-state laser pumping, and spectroscopy. Diffraction-limited high-power diode lasers have been available from the red to the near infrared spectral range since the introduction of tapered diode laser technique, where a narrow-stripe ridge-waveguide (RW) section ensures a diffraction-limited emission, and a tapered amplifier (TA) section allows high output power [1-3]. The techniques to achieve narrow-linewidth emission by etching a grating in the semiconductor material, such as the distributed feedback (DFB) or distributed Bragg reflector (DBR) feedback techniques, are well developed for tapered diode lasers in the near infrared from 900 to 1200 nm [3-5]. These techniques are not mature around 808 nm, and no DBR or DFB tapered diode lasers around 808 nm are commercially available, to the best of our knowledge. One reason of the failure of these techniques at 808 nm is the property of the internal grating in the tapered diode laser is not stable, thus the lifetime of the laser device is short. One application of the narrow-linewidth and diffraction limited 808 nm diode laser is the generation of high-power 404 nm UV light by single-pass frequency doubling. For this application, the 808 nm diode laser with a watt-level output power is desired, and the linewidth should be less than 10 pm.

To achieve narrow-linewidth tapered diode laser modules around 808 nm, various methods have been suggested. The methods mainly used fall into two categories: (1) injection locking to an external single-mode master laser (also called master-oscillator power-amplifier, MOPA) [6-8], or (2) external-cavity feedback with a frequency selective element [9-12]. The second approach is preferred since the additional single-mode master oscillator is not needed. In that approach, different frequency-selective elements are implemented to achieve a narrow-linewidth tapered diode laser system, e.g., bulk diffraction gratings [11,13], fiber Bragg gratings [9,14], narrowband interference filters [15], phase conjugate mirrors [10] and volume Bragg gratings (VBGs) [12,16]. VBGs based on photosensitive glasses are key elements for achieving a compact and relatively temperature insensitive wavelength-stabilized narrow-linewidth diode laser [17]. They have been widely used to stabilize the wavelength of diode laser systems with broad-area diode lasers [18,19], broad-area diode laser arrays [20,21], tapered diode lasers [12,16] and tapered diode laser bars [22,23]. VBGs have also been used to combine DBR-tapered diode lasers around 1060 nm, and the combined laser system was used to generate green light [24].

Around 808 nm, a tunable narrow-linewidth external-cavity tapered diode laser system based on a bulk diffraction grating was demonstrated with a maximum output power around 2.0 W [11]. Based on a VBG, a wavelength stabilized external-cavity tapered diode laser was achieved with an output power of 2.5 W, a narrow linewidth (< 20 pm) and, a beam propagation factor M^2 of less than 4 [12]. However, for both cases the optical elements, such as collimating lenses and gratings, were mounted on bulky optomechanical components separate from the gain medium. In addition, tapered amplifiers with a single electrical contact were used, limiting injection current related adjustments of the spatial quality [25].

Here, we demonstrate a compact micro-integrated external-cavity diode laser (ECDL) system based on a tapered amplifier with two separated electrical contacts and a VBG. The tapered amplifier, collimating lenses and the grating are micro-integrated on a 5 mm x 13 mm aluminum nitride micro-optical bench on a conduction cooled package (CCP) mount with a footprint of 25 mm x 25 mm. An output power of up to 3.5 W is obtained with an emission linewidth of less than 6 pm, limited by the resolution of the optical spectrum analyzer, and an M^2 value in the slow axis of 2.6.

2. MICRO-INTEGRATED ECDL at 808 NM: OPTICAL AND MECHANICAL DESIGN

Fig. 1 shows a scheme of the optical concept applied for the ECDL. A tapered amplifier is used as gain medium. Its vertical layer structure is grown by low-pressure metal–organic vapor phase epitaxy and is based on a GaAsP single quantum well embedded in a 3 µm thick AlGaAs waveguide. The resulting vertical far field angle of 18° measured at full width at half maximum (FWHM) enables an easy beam shaping.

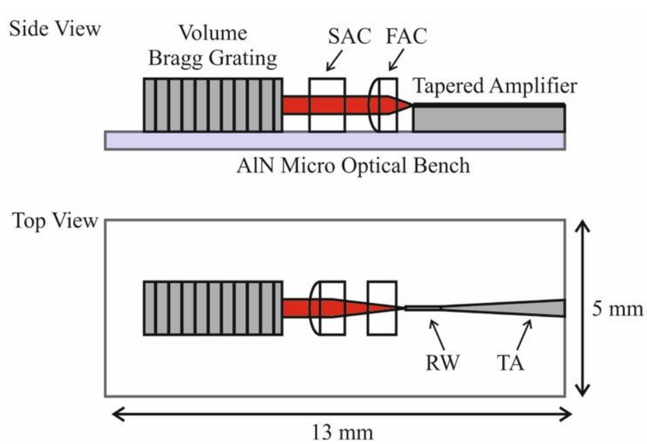

Fig. 1. Scheme of the optical concept for a micro-integrated external-cavity tapered diode laser. FAC, fast axis collimating lens; SAC, slow axis collimating lens.

The 4 mm device consists of a 1 mm long, 3 µm wide ridge waveguide and a 3 mm long tapered amplifier with a full angle of 6°. Waveguide and amplifier can be operated individually. Both facets are anti-reflection coated with reflectivities of 0.5% at the front and smaller than 10^{-4} at the rear facet. The vertical layer structure of the gain medium and a figure of the tapered device have been published in Ref. 3.

The device is mounted p-side up on a copper tungsten submount on a 5 mm x 13 mm aluminum nitride micro-optical bench. Micro cylindrical lenses (Ingeneric GmbH) are used for collimation of the rear side waveguide emission in the fast axis (FAC) and slow axis (SAC). Both optics are selected based on optical simulations. For vertical fast axis collimation a lens with a focal length of $f = 0.6$ mm and a numerical aperture of NA = 0.8 is used. The lens dimensions are L x W x H = 0.8 x 1.5 x 1.0 mm³. Lateral slow axis collimation is realized with a lens with $f = 2.3$ mm, NA = 0.3 and dimensions of L x W x H = 1.0 x 1.5 x 1.5 mm³.

A reflecting VBG (OptiGrate Corp) is used as a wavelength selective rear side cavity mirror. The resulting resonator of the external cavity diode laser stretches from the front facet of the tapered amplifier to the grating. At a central wavelength of 808 nm, the grating has a spectral selectivity of 0.15 nm (FWHM) and a diffraction efficiency larger than 90%. Its dimensions are L x W x H = 3.9 x 1.5 x 2.5 mm³. The distance between the rear facet and the grating is about 4 mm. Considering the length of the tapered device/lenses and their corresponding refractive indexes, the longitudinal mode space of the ECDL is around 12 pm. All optical components are mounted onto the micro-optical bench using an UV curable adhesive. The compact subassembly is mounted on a 25 mm x 25 mm CCP mount. The micro-integrated ECDL is mounted on a copper base plate for the characterization, which is temperature stabilized at 20°C during the characterization, unless otherwise specified.

3. RESULTS AND DISCUSSION

The micro-integrated ECDL at 808 nm is characterized by scanning the injection current to the ridge-waveguide section (I_{RW}) and to the tapered amplifier section (I_{TA}) with steps of 25 and 50 mA, respectively. The highest I_{RW} and I_{TA} used in the experiment are 0.2 and 6.0 A, respectively, to avoid damage. The output power of the laser system is measured with a power meter (Ophir, Nova) and the spectrum of the output beam is recorded with an optical spectrum analyzer (Advantest Corp. Q8347).

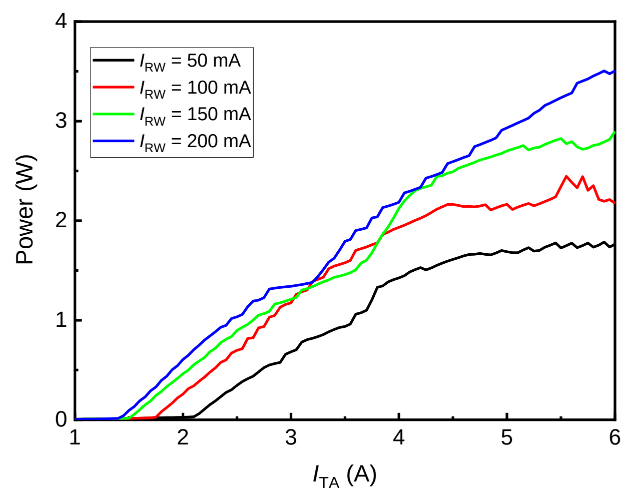

Fig. 2. Optical output power versus injection current to the tapered amplifier section I_{TA}, with the currents to the ridge-waveguide section I_{RW} of 50, 100, 150 and 200 mA.

Figure 2 shows the output power of the micro-integrated ECDL with different injected I_{TA} when I_{RW} is 50, 100, 150 and 200 mA. As expected, the threshold current decreases with higher I_{RW}, it is decreased from 2.1 A when I_{RW} = 50 mA to 1.4 A when I_{RW} = 200 mA. The output power increases with I_{TA}, but is saturated at high I_{TA} when I_{RW} is low (< 100 mA). The corresponding slope efficiencies measured up to 1 W of output power are in the range of 0.9-1.0 W/A at $I_{RW} \geq 100$ mA. At I_{RW} = 50 mA a reduction to 0.6 W/A is observed. The maximum output power is around 1.75 W at I_{RW} = 50 mA, while it increases to 3.50 W at I_{RW} = 200 mA.

The peak emission wavelength of the spectrum of the output beam from the micro-integrated ECDL as a function of the injected currents I_{RW} and I_{TA} is measured. Generally, the peak wavelength increases with the injected current I_{TA}, but the increase is not monotonous. The peak wavelength is stabilized in the range of 0.14 nm centered at 808.27 nm with all the different injected currents to ridge-waveguide section and tapered amplifier section. This stabilized peak wavelength range corresponds to the 0.15 nm spectral bandwidth of the VBG.

The normalized spectra of the micro-integrated ECDL with different injected current I_{TA} at I_{RW} = 200 mA are shown in Fig. 3. For most of the injection current I_{TA}, single mode operation is observed. In the I_{TA} range around 2.4 to 3.1 A, the spectra show multimode operation. Insets show these two kinds of typical emission spectra extracted from Fig. 3. The emission spectrum of the micro-integrated ECDL with I_{TA} of 2.9 A in inset (a) shows three main peaks, and a FWHM spectral bandwidth of 59 pm. The output power in this case is 1.33 W. The emission spectrum of the micro-integrated ECDL with I_{TA} of 6.0 A in inset (b) shows one narrow peak with a FWHM spectral linewidth of 6 pm, corresponding to the resolution limit of the optical spectrum analyzer. The output power in this case is 3.50 W.

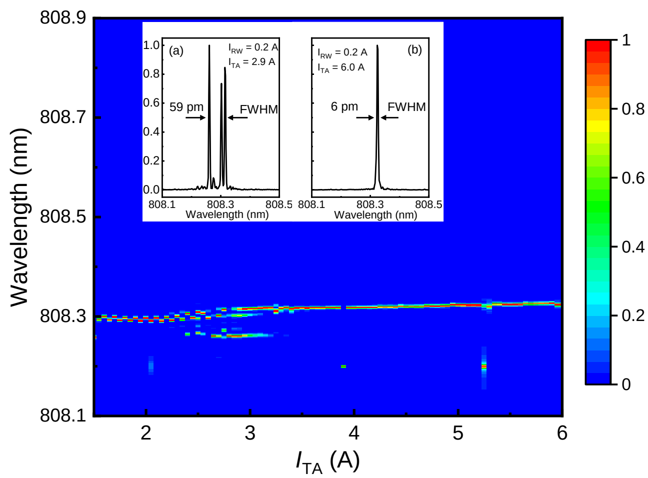

Fig. 3. False color plot of the normalized spectra of the micro-integrated ECDL as a function of I_{TA} with measurement steps of 50 mA, at an I_{RW} of 200 mA. Insets, emission spectra of the micro-integrated ECDL with multimode operation at 1.33 W (a) and single mode operation at 3.50 W (b)

The peak wavelength of the micro-integrated ECDL is determined by the central wavelength of the VBG, λ_c. The ECDL operates at a single longitudinal mode m which is in the closest spectral vicinity to λ_c. When the injected current I_{TA} is low (< 2.4 A), as the increase of I_{TA}, the self-heating and the temperature-induced increase of the refractive index of the tapered amplifier will cause the wavelength of each mode a red shift. Thus the ECDL will jump to oscillate at a higher order longitudinal mode which is closest to λ_c, this the reason of the fluctuation of the peak wavelength around λ_c within the mode spacing of the ECDL when I_{TA} < 2.4 A. As the I_{TA} increases further, the self-heating effect also affects the VBG and the collimating lenses, thus the central wavelength of the VBG, λ_c, also increases with I_{TA}. The effect of self-heating on tapered amplifier, VBG and lenses makes the ECDL system unstable and in multimode operation. When I_{TA} >3.1 A, the micro-integrated ECDL operates stably in single longitudinal mode again. The peak wavelength of the ECDL increases very slowly with I_{TA}, due to the red shift of λ_c induced by self-heating effect. However, the reason of the two big jumps to shorter wavelengths at I_{TA} of 3.9 and 5.25 A is still under investigation.

The beam quality of the output beam from the micro-integrated ECDL system is evaluated by measuring the beam propagation factor M^2 in both fast and slow axis directions. The M^2 factor (1/e^2) is measured with a beam propagation analyzer (Spiricon, M^2-200s-FW) at different output power levels for an injection current I_{RW} of 0.2 A. Fig. 4 shows the measured M^2 for both fast and slow axis directions. For the fast axis direction, the M^2 value is around 1.3 at all output powers. For the slow axis direction, the M^2 value is less than 1.5 at low output power, while it tends to increase with output power. At the maximum output power of 3.5 W, the M^2 value in the slow axis direction is 2.6.

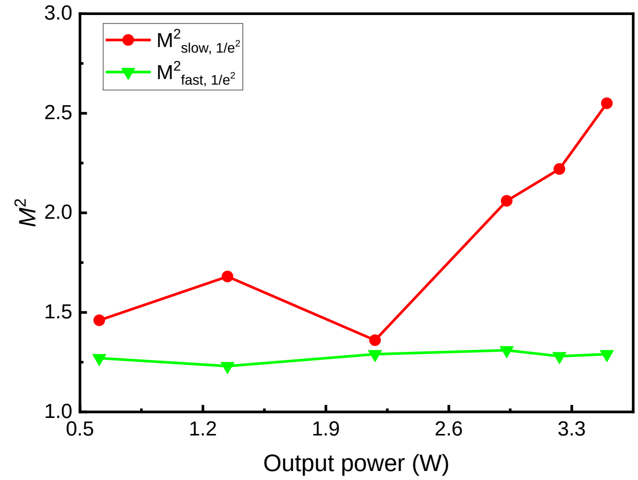

Fig. 4. Beam propagation factor M^2 for both the fast and slow axis directions of the micro-integrated ECDL vs the output power at I_{RW} = 0.2 A.

For an ordinary non-wavelength stabilized diode laser emitting around 800 nm, the wavelength increases with temperature is around 0.3 nm/K [18]. This is mainly due to the change of the bandgap and the corresponding shift of the optical gain spectrum of the gain medium with temperature, while the increase of refractive index and thermal expansion of semiconductor material only has minor influence [26]. For diode lasers with internal grating feedback, such as DBR diode laser, the wavelength shift with temperature at 785 nm is around 0.06 nm/K [27], around one fifth of that of a Fabry-Perot diode laser. One advantage of using a VBG as an external-cavity feedback element is that the wavelength of the ECDL is less dependent on the temperature of the gain medium.

The normalized spectrum of the micro-integrated ECDL is measured at different temperatures from 15 to 30°C with a step size of 1°C. The injection currents of I_{RW} and I_{TA} are 125 mA and 3.2 A, respectively. The spectra show a single peak profile with a spectral linewidth at the resolution limit of 6 pm throughout the whole temperature range. Fig. 5 plots the peak emission wavelength of the spectra and the output power of the micro-integrated ECDL as a function of the base plate temperature. The peak wavelength increases from 808.259 nm at 15°C to 808.354 nm at 30°C, corresponding to an increasing rate of 6.5 pm/K, typical for the applied grating. This is around one order of magnitude lower than that for a typical DBR diode laser. The central wavelength of the reflecting grating (DBR or VBG) is proportional to the product of the refractive index of the material and the grating period [17]. Therefore, two effects influence the central wavelength of the gratings. First, the thermo-optic effect by influencing the refractive index, and second, the thermal expansion by affecting the grating period. For a DBR grating based on AlGaAs, the influence of the thermal expansion is negligible compared with that of the thermo-optic effect [28]. For a VBG based on photosensitive glass, in contrast, the influence of the thermo-optic effect is negligible compared with that of the thermal expansion [29]. The influence of the thermo-optic effect on a DBR grating is around one order of magnitude higher than the effect of the thermal expansion on a VBG [28,29]. This is the reason that the wavelength of the ECDL based on a VBG is much more stable when the operating temperature is increased. Fig. 5 also shows that the output power decreases from 1.43

W at 15°C to 1.17 W at 30°C, corresponding to a decrease of 17.2 mW/K. Each peak on the power vs. temperature curve corresponds to a longitudinal mode hop to a higher order mode. This is also consistent with a relatively big step increase of the emission wavelength [26].

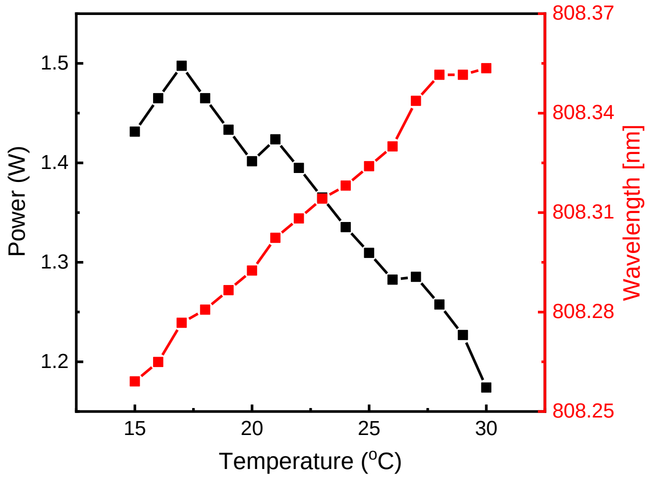

Fig. 5. Output power and peak emission wavelength of the micro-integrated ECDL as a function of operating temperature, with I_{RW} of 125 mA and I_{TA} of 3.2 A.

The micro-integrated ECDL technique based on a VBG presented here is valid from UV (350 nm) to near infrared (2.5 µm) spectral range. Compared with other techniques, the compactness and temperature insensitive emission wavelength of the micro-integrated ECDL are the main advantages. These advantages make the ECDLs attractive for many applications, such as nonlinear frequency conversion and spectroscopy. For the applications of spectroscopy and laser cooling, a diode and fiber hybrid laser system is widely used, where a tunable narrow-linewidth diode laser is used as a master oscillator, and the output power of the diode laser is boosted by a fiber amplifier [30]. Compared with the hybrid laser system, the micro-integrated ECDL is more simplicity and compactness, the output power is comparable and the wavelength can be tuned by the temperature in a limiting range. The measured 6 pm linewidth of the micro-integrated ECDL limited by the resolution of the spectrum analyzer is not narrow enough for spectroscopic application. A more accurate approach, such as the delayed self-heterodyne interferometer method or an unbalanced-path Mach-Zehnder interferometer method, should be used to characterize the linewidth further [31].

4. CONCLUSION

A micro-integrated ECDL based on a tapered diode amplifier and a VBG at 808 nm is demonstrated. All the components are integrated on a 5 mm x 13 mm aluminum nitride micro-optical bench on a CCP mount with a footprint of 25 mm x 25 mm. As high as 3.5 W output power is achieved with an upper bound of spectral linewidth of 6 pm and an M^2 value of 2.6 in the slow axis. The emission wavelength of the ECDL is temperature stabilized and increases with a rate of 6.5 pm/K, typical for the applied grating. The micro-integrated ECDL system has potential applications in many fields, such as frequency doubling to UV light, where a compact narrow-linewidth, high-power, diffraction-limited laser around 808 nm is needed.

Funding Information. Eurostars (E! 11592 – CPILS)

Disclosures. The authors declare no conflicts of interest.

References

1. S. O'Brien, D. F. Welch, R. A. Parke, D. Mehuys, K. Dzurko, R. J. Lang, R. Waarts, and D. Scifres, "Operating characteristics of a high-power monolithically integrated flared amplifier master oscillator power amplifier," IEEE J. Quantum Electron. **29,** 2052-2057 (1993).
2. H. Wenzel, B. Sumpf and G. Erbert, "High-brightness diode lasers," C. R. Physique **4**, 649-661 (2003).
3. B. Sumpf. K.-H. Hasler, P. Adamiec, F. Bugge, F. Dittmar, J. Fricke, H. Wenzel, M. Zorn, G. Erbert and G. Tränkle, "High-brightness quantum well tapered lasers," IEEE J. Sel. Topics Quantum Electron. **15**, 1009-1020 (2009).
4. A. Müller, C. Zink, J. Fricke, F. Bugge, G. Erbert, B. Sumpf and G. Tränkle, "Efficient, high brightness 1030 nm DBR tapered diode lasers with optimized lateral layout," IEEE J. Sel. Topics Quantum Electron. **23**, 1501107 (2017).
5. B. Sumpf and K. Paschke, "Spectrally stabilized high-power high-brightness DBR-tapered lasers in the VIS and NIR range," Proc. SPIE **10518**, 1051817 (2018).
6. A. C. Wilson, J. C. Sharpe, C. R. McKenzie, P. J. Manson and D. M. Warrington, "Narrow-linewidth master-oscillator power amplifier based on a semiconductor tapered amplifier," Appl. Opt. **37**, 4871-4875 (1998).
7. M. Schiemangk, K. Lampmann, A. Dinkelaker, A. Kohfeldt, M. Krutzik, C. Kürbis, A. Sahm, S. Spieβberger, A. Wicht, G. Erbert, G. Tränkle and A. Peters, "High-power, micro-integrated diode laser modules at 767 and 780 nm for portable quantum gas experiments," Appl. Opt. **54**, 5332-5338 (2015).
8. E. Ji, Q. Liu, M. Nie, X. Fu and M. Gong, "Theoretical and experimental analysis of high-power frequency-stabilized semiconductor master oscillator power-amplifier system," App. Opt. **55**, 2909-2914 (2016).
9. A. K. Goyal, P. Gavrilovic and H. Po, "1.35 W of stable single-frequency emission from an external-cavity tapered oscillator utilizing fiber Bragg grating feedback," Appl. Phys. Lett. **73**, 575-577 (1998).
10. C. Pedersen and R. S. Hansen, "Single frequency, high power, tapered diode laser using phase-conjugated feedback," Opt. Express **13**, 3961-3968 (2005).
11. M. Chi, O. B. Jensen, J. Holm, C. Pedersen, P. E. Andersen, G. Erbert, B. Sumpf and P. M. Petersen, "Tunable high-power narrow-linewidth semiconductor laser based on an external-cavity tapered amplifier," Opt. Express **13**, 10589-10596 (2005).
12. G. Lucas-Leclin, D. Paboeuf, P. Georges, J. Holm, P. Andersen, B. Sumpf and G. Erbert, "Wavelength stabilization of external-cavity tapered lasers with volume Bragg gratings," Appl. Phys. B **91**, 493-498 (2008).
13. M. Chi, G. Erbert, B. Sumpf and P. M. Petersen, "Tunable high-power narrow-spectrum external-cavity diode laser based on tapered amplifier at 668 nm," Opt. Lett. **35**, 1545-1547 (2010).
14. K. Sakai, S. Itakura, N. Shimada, K. Shibata, Y. Hanamaki, T. Yagi and Y. Hirano, "High-power tapered unstable-resonator laser diode with a fiber-Bragg-grating reflector," IEEE Photon. Technol. Lett. **21**, 1103-1105 (2009).
15. Y. Huang, D. N. Patel, T. Chen, Y. Huang, Y. Chan, C. Nauer, Y. Liu, Li-Wang and J. Shy, "Watt-level single-frequency tapered amplifier laser using a narrowband interference filter," Appl. Opt. **57**, 7038-7044 (2018).
16. T. Tien, M. Maiwald, B. Sumpf, G. Erbert and Tränkle, "Microexternal cavity tapered lasers at 670 nm with 5 W peak power and nearly diffraction-limited beam quality," Opt. Lett. **33**, 2692-2694 (2008).
17. G. Steckman, W. Liu, R. Platz, D. Schroeder, C. Moser and F. Havermeyer, "Volume holographic grating wavelength stabilized laser diodes," IEEE J. Sel. Topics Quantum Electron. **13**, 672-678 (2007).
18. B. L. Volodin, S. V. Dolgy, E. D. Melnik, E. Downs, J. Shaw and V. S. Ban, "Wavelength stabilization and spectrum narrowing of high-power multimode laser diodes and arrays by uses of volume Bragg grating," Opt. Lett. **29**, 1891-1893 (2004).

19. M. Niebuhr, C. Zink, A, Jechow, A. Heuer, L. B. Glebov and R. Menzel, "Mode stabilization of a laterally structured broad area diode laser using an external volume Bragg grating," Opt. Express **23**, 12394-12400 (2015).
20. B. Liu, X. Tong, C. Jiang, D. R. Brown and L. Robertson, "Development of stable, narrow spectral line-width, fiber delivered laser source for spin exchange optical pumping," App. Opt. **54**, 5420-5424 (2015).
21. B. Liu and Y. Braiman, "Coherent addition of high power broad-area laser diodes with a compact VBG V-shaped external Talbot cavity," Opt. Commun. **414**, 202-206 (2018).
22. I. Hassiaoui, N. Michel, G. Bourdet, R. Mc Bride, M. Lecomte, O. Parillaud, M. Calligaro, M. Krakowski and J.-P. Huignard, "Very compact external cavity diffraction-coupled tapered laser diodes," Appl. Opt. **47**, 746-750 (2008).
23. D. Paboeuf, G. Lucas-Leclin, P. Georges, N. Michel, M. Krakowski, J. Lim, S. Sujecki and E. Larkins, "Narrow-line coherently combined tapered laser diodes in a Talbot external cavity with a volume Bragg grating," Appl. Phys. Lett. **93**, 211102 (2008).
24. A. Müller, O. B. Jensen, K.-H. Hasler, B. Sumpf, G. Erbert, P. E. Andersen and P. M. Petersen, "Efficient concept for generation of diffraction-limited green light by sum-frequency generation of spectrally combined tapered diode laser," Opt. Lett. **37**, 3753-3755 (2012).
25. H. Odriozola, J. M. G. Tijero, L. Borruel, I. Esquivias, H. Wenzel, F. Dittmar, K. Paschke, B. Sumpf, and G. Erbert, "Beam Properties of 980-nm Tapered Lasers With Separate Contacts: Experiments and Simulations," IEEE J. Quantum Electron. **45,** 42 (2009).
26. P. Unger, "Introduction to power diode laser," in *High-power diode lasers, Fundamentals, Technology, Applications*, R. Diehl, ed. (Springer-Verlag Berlin Heidelberg, 2000), pp. 31-34.
27. A. Müller, M. Maiwald, and B. Sumpf, "Compact diode laser-based dual-wavelength master oscillator power amplifier at 785 nm," IEEE Photon. Technol. Lett. **31**, 1120-1123 (2019).
28. J. P. Kim and A. M. Sarangan, "Temperature-dependent Sellmeier equation for the refractive index of $Al_xGa_{1-x}As$," Opt. Lett. **32**, 536-538 (2007).
29. N. Nikonorov, V. Aseev, V. Dubrovin, A. Ignatiev, S. Ivanov, Y. Sgibnev and A. Sidorov, "Photonic, plasmonic, fluidic, and luminescent devices based on new polyfunctional photo-thermo-refractive glass," in *Optics, photonics and laser technology*, P. A. Ribeiro and M. Raposo, ed. (Springer Nature Switzerland AG, 2018), pp. 93-97.
30. D. K. Shin, B. M. Henson, R. I. Khakimov, J. A. Ross, C. J. Dedman, S. S. Hodgman, K. G. H. Baldwin, and A. G. Truscott, "Widely tunable, narrow linewidth external-cavity gain chip laser for spectroscopy between 1.0 – 1.1 µm," Opt. Express **24**, 27403-27414 (2016).
31. S. Bennetts, G. D. McDonald, K. S. Hardman, J. E. Debs, C. C. N. Kuhn, J. D. Close and N. P. Robins, "External cavity diode lasers with 5 kHz linewidth and 200 nm tuning range at 1.55µm and methods for linewidth measurement," Opt. Express **22**, 10642-10654 (2014).